8

Research Article

Yihong Li, Yukun Zhao, and Huiqin Chen*

Prediction model of interfacial heat transfer coefficient changing with time and ingot diameter

https://doi.org/10.1515/htmp-2022-0008 received December 09, 2021; accepted December 29, 2021

Abstract: We established and simulated finite element solidification models of ingots with 180, 380, 800, 1,300, and 1,880 mm diameters, and the solidification process temperature distributions for the five ingot sizes were assessed by Fluent. On this basis, we established a mathematical model for the interfacial heat transfer coefficient between the ingot and the ingot mold, as well as the ingot diameter and solidification time, using the regression analysis method. The results showed that the change law for the interfacial heat transfer coefficients of the ingots with different sizes and times conformed to the change law of the exponential function, and the interfacial heat transfer coefficient and the ingot diameter had a linear relationship. The interfacial heat transfer coefficient, based on a measured temperature of about 36 tons of ingot with an average diameter of 1,500 mm and about 8.5 tons of ingot with an average diameter of 820 mm, was compared to the interfacial heat transfer coefficient calculated by the model. We found that the variation law of the two was essentially the same, indicating that this model could correctly reflect the interfacial heat transfer coefficient between the ingot and the ingot mold in the literature.

Keywords: ingots, interfacial heat transfer coefficient, numerical simulation, prediction model

Yukun Zhao: School of Materials Science and Engineering, Taiyuan University of Science and Technology, Taiyuan 030024, China, e-mail: 1276570032@qq.com

1 Introduction

The solidification process of steel ingots has several issues, including complex heat transfer and flow, and visualizing the high-temperature casting process using existing physical methods is difficult. In recent years, with improved computer technology, numerical simulations of the casting process have become an important way to optimize the design of steel ingots for casting. The interfacial heat transfer coefficient is a boundary condition that must be set for numerical simulations, and its accuracy significantly affects the accuracy of the simulation results. Therefore, many researchers have conducted a significant amount of research on the heat transfer coefficient of the ingot—mold interface.

Li et al. [1] used a new experimental system to measure simultaneously displacement and temperature in a 23 kg steel ingot and ingot mold during solidification, and inversed the interfacial heat transfer coefficients from the measuring results by using an inverse heat conduction model. The results showed that the heat conduction of the air gap accounts for about 70% of effectiveness when the gap is large. Muojekw et al. [2] studied the effects of mold materials on the interfacial heat transfer coefficient, and the results showed that the interfacial heat transfer coefficient increased with increasing thermal diffusivity of the mold materials. Kumar and Prabhu [3] studied the influence of different material coatings on the interfacial heat transfer coefficient, and the results indicated that the coating reduced the interfacial heat transfer coefficient. The researchers found that the interfacial heat transfer coefficient of the aluminum-based coating was larger than that of a refractory coating with the same thickness. Lan and Zhang [4] from the University of Science and Technology Beijing simulated and analyzed the variations in air gap widths and the interfacial heat transfer coefficients at different positions during the pouring process of 8.5 tons of ingot [5]. The results showed that the maximum heat flux and heat transfer coefficient values

International License.

^{*} Corresponding author: Huiqin Chen, School of Materials Science and Engineering, Taiyuan University of Science and Technology, Taiyuan 030024, China, e-mail: S20190358@stu.tyust.edu.cn Yihong Li: School of Materials Science and Engineering, Taiyuan University of Science and Technology, Taiyuan 030024, China, e-mail: 2015016@tyust.edu.cn

were located at 1/4 width during the beginning of solidification, and the heat transfer coefficient of the wide surface was slightly larger than that of the narrow surface. Zeng et al. [6] studied the effects of the width of the air gap and the duration of gap formation on interfacial heat transfer coefficient by experiment and inverse calculation. The results showed that the interfacial heat transfer coefficient decreased as gap width increased and the duration of gap formation increased. Guo et al. [7] studied the effects of molds with different thicknesses on the interfacial heat transfer coefficient, and the results showed that the thicker the mold, the smaller the interfacial heat transfer coefficient. Li et al. [8], Shen et al. [9], and Liu et al. [10] selected interfacial heat transfer coefficients ranging from 150 to 1.500 W/(m².°C) for pouring and solidification simulations of large steel ingots. This simplified treatment significantly improved the calculation efficiency but greatly affected the accuracy of the results [11].

In the literature, the variation law of interfacial heat transfer coefficient of ingots with different sizes is quite different. Therefore, it is difficult to use the variation of heat transfer coefficient from other reports in the literature, for solidification temperature field simulations. In this study, the three-dimensional models of ingots with different sizes are established, the variation law of interfacial heat transfer coefficient between ingots and ingot molds with different sizes is analyzed by fluent finite element analysis software, and the mathematical model between interfacial heat transfer coefficient and ingot diameter and solidification time is established by mathematical regression method.

2 Interfacial heat transfer coefficient model

2.1 Heat transfer mode of solidification

The heat transfer process between the ingot and the ingot mold after the completion of ingot casting is very complex. In addition, there are three heat transfer modes: heat conduction between the ingot and the ingot mold, heat convection between the molten steel and the ingot mold, and heat radiation from the ingot to the ingot mold [12]. The expression of the thermal resistance is as follows:

$$\frac{1}{R_{\text{total}}} = \frac{1}{R_{\lambda}} + \frac{1}{R_{\alpha}} + \frac{1}{R_{\text{h}}} = \frac{\lambda A}{s} + \alpha A + \alpha_{\text{h}} A, \quad (1)$$

where R_{total} , R_{λ} , R_{α} , and R_{h} are the thermal resistance parameters (°C/W), λ , α , and α_{h} denote the air thermal conductivity, convective heat transfer coefficient between the molten steel and the ingot mold, and the radiation heat transfer coefficient from the ingot to the ingot mold, respectively (in W/(m².°C)), λ can be obtained by referencing the physical properties of dry air under atmospheric pressure, s is the air gap thickness (mm), and A is the heat transfer area (m²).

The expression of the thermal resistance per unit area is as follows:

$$\frac{1}{r_{\text{total}}} = \frac{1}{r_{\lambda}} + \frac{1}{r_{\alpha}} + \frac{1}{r_{\text{h}}} = \frac{\lambda}{s} + \alpha + \alpha_{\text{h}}, \tag{2}$$

where r_{total} , r_{λ} , r_{α} , and r_{h} are the thermal resistance parameters per unit area ((m².°C)/W).

The interfacial heat transfer coefficient can be obtained by adding the heat transfer coefficient contribution of the air gap, the convection heat transfer coefficient, and the radiation heat transfer coefficient parameters as follows:

$$h = \frac{1}{r_{\text{total}}} = \frac{\lambda}{s} + \alpha + \alpha_{\text{h}}, \tag{3}$$

where h is the comprehensive interfacial heat transfer coefficient (W/(m^2 . $^{\circ}$ C)).

After pouring the molten steel, the ingot temperature gradually declines and the ingot will begin to solidify and shrink. As a result, an air gap between the ingot and the ingot mold will form; thus, the ingot and ingot mold will no longer be in direct contact. Also, heat transfer between the ingot and the ingot mold can occur in two main ways: thermal radiation and heat conduction of the air in the air gap. The interfacial heat transfer coefficient can be obtained by adding the heat transfer coefficient contribution of the air gap and the radiation heat transfer coefficient as follows:

$$h = \frac{1}{r_{\text{total}}} = \frac{\lambda}{s} + \alpha_{\text{h}}.$$
 (4)

2.2 Determination of the interfacial heat transfer coefficient

2.2.1 Coefficient of convective heat transfer

The convective heat transfer coefficient can be determined as follows:

$$\alpha \equiv \frac{\lambda_1 N u}{L},\tag{5}$$

where λ_1 is the thermal conductivity of the molten steel (W/(m².°C)), L is the characteristic length (m), and Nu is the Nusselt number.

The Nusselt number can be determined as follows:

$$Nu = C(Gr \cdot Pr)^n, \tag{6}$$

where Gr is the Grashof number, Pr is the Prandtl number, C is 0.59, and n is 1/4.

The Grashof number can be determined as follows:

$$Gr = \frac{g\beta\Delta TL^3}{v^2},\tag{7}$$

where g is the acceleration of gravity (9.81 m/s²), β is the volume expansion coefficient, ν is the kinematic viscosity (m²/s), and ΔT is the temperature difference between ingot and ingot mold.

The Prandtl number can be determined as follows:

$$Pr = \frac{\mu c_{p}}{\lambda_{1}},$$
 (8)

where μ is the dynamic viscosity (Pa/s) and $c_{\rm p}$ is the specific heat capacity.

2.2.2 Radiation heat transfer coefficient

The expression of the heat flux q_h and heat transfer coefficient α_h for radiation heat transfer at the ingot moldingot interface is as follows:

$$q_{\rm h} = \frac{\sigma(T_1^4 - T_2^4)}{\frac{1}{\varepsilon_1} + \frac{1}{\varepsilon_2} - 1},\tag{9}$$

$$\alpha_{\rm h} = \frac{q_{\rm h}}{T_1 - T_2}.\tag{10}$$

The expression of that radiation heat transfer coefficient of the mold-ingot interface by transforming equations (9) and (10) is as follows:

$$\alpha_{\rm h} = \frac{\sigma(T_1^2 + T_2^2)(T_1 + T_2)}{\frac{1}{c_1} + \frac{1}{c_2} - 1},$$
 (11)

where σ is the Stephen–Boltzmann constant of 5.67 × 10⁻⁸ W/(m²·K⁴), and ε_1 ε_2 are the surface emissivity of the ingot and the mold, respectively (ε_1 = 0.9, ε_2 = 0.85).

2.2.3 Heat transfer coefficient of air gap contribution

The expression of the heat flux generated by the gas heat conduction of the air gap at the ingot—die interface is as follows:

$$q_{\rm c} = \lambda \frac{T_1 - T_2}{\rm s} A,\tag{12}$$

where *A* is the heat transfer area (m²), λ is the gas thermal conductivity (W/(m^{2.o}C)), and *s* is the air gap thickness (mm).

The interfacial heat transfer coefficient $\frac{\lambda}{s}$ of the air gap contribution could then be derived as follows:

$$\frac{\lambda}{s} = \frac{q_{\rm c}}{A(T_1 - T_2)}.\tag{13}$$

Mustafa et al. [13] measured the thickness of the air gap between the ingot and the ingot mold during the solidification of 10 tons of ingot, which solidified in a $762 \text{ mm} \times 889 \text{ mm} \times 2,565 \text{ mm}$ mold. The measurement results showed that the air gap thickness s in the middle of the wide surface was approximately linear with time t, as shown in equation (14). The variation in air gap thickness in this work was calculated as follows:

$$s = 0.000388101t + 0.020741,$$
 (14)

where *t* is the solidification time (s).

2.3 Analog calculations

Based on the abovementioned theoretical methods, and using the initial ingot and ingot mold conditions, we calculated the three heat transfer coefficients for heat conduction, convection, and radiation. The sum of these three heat transfer coefficients was used as the initial interfacial heat transfer coefficient, which was then input to Fluent software as the initial boundary condition. After the calculation starts, the temperature of the ingot and the ingot mold is recorded every fixed time period, and the heat transfer coefficient at this moment is calculated and input to the software as the boundary condition for the next time period.

2.3.1 Geometric model

The 3D modeling software DesignModeler in Workbench is used to create three-dimensional (3D) ingot models, with diameters of 180, 380, 800, 1,300, and 1,880 mm and a height of 1,000 mm. The mesh grid division tool was used to mesh the model. Figure 1 shows the 800 mm diameter model of the ingot and the corresponding ingot mold.

2.3.2 Basic model assumptions

Because the ingot solidification process is very complex with many influencing factors, it was necessary to make some reasonable simplifications to the model for the actual simulation process, as well as to ignore some factors that had minimal influence on the simulation results. Using this approach, the simulation results were still close to the actual results in the simulation, the model was simplified as follows [14]:

- The liquid metal instantaneously filled with ingot mold, and the initial temperature of the liquid metal was the pouring temperature.
- 2. The thermal properties of the molten steel and ingot mold were set as constants.
- 3. Without considering the solute migration and undercooling phenomenon, the liquid steel started to solidify when it cooled to the liquid temperature [15].

2.3.3 Heat-transport equation

The heat-transport equation is given by

$$\rho c \frac{\partial T}{\partial t} = \frac{\partial}{\partial x} \left(k \frac{\partial T}{\partial x} \right) + \frac{\partial}{\partial y} \left(k \frac{\partial T}{\partial y} \right) + \frac{\partial}{\partial z} \left(k \frac{\partial T}{\partial z} \right). \tag{15}$$

The latent heat of solidification in the model is treated as follows:

$$HT = \int_{0}^{T} c_{p} dT + L(1 - f_{s}), \qquad (16)$$

and derivation of equation (16) gives



Figure 1: Model of the 800 mm diameter ingot and the ingot mold.

$$c = c_p - L \frac{\mathrm{d}f}{\mathrm{d}T},\tag{17}$$

where c is the effective specific heat capacity, L is the latent heat of solidification, and f_s is the solid fraction.

2.3.4 Material parameters

(Table 1).

2.3.5 Initial conditions

- 1. The ambient temperature was 27°C (300 K).
- 2. The pouring temperature of the molten steel was 1,560°C (1,833 K).

2.3.6 Boundary conditions

- 1. The adiabatic surface between the molten steel and the slag was set, assuming that the molten steel surface was covered by a layer of slag.
- 2. The heat transfer coefficient at the bottom of the ingot mold was set to $20 \text{ W/(m}^2 \cdot ^{\circ}\text{C})$.
- 3. The heat transfer coefficient between the sidewall of the ingot mold and the air was set to $50 \text{ W/(m}^2 \cdot ^{\circ}\text{C})$.
- 4. The interfacial heat transfer coefficient is calculated from the temperature of the ingot and ingot mold in the previous time period.

2.4 Simulated results

The positions of points 1 and 2 at one-half of the ingot height were the temperature measurement points, as shown in Figure 2.

Table 1: Thermophysical parameters of molten steel [16]

Physical quantity	Unit	Parameter value
Density of the ingots	kg/m³	7,800
Density of the molten steel	kg/m³	7,500
Specific heat capacity	$J/(kg^{-1}\cdot K^{-1})$	720
Thermal conductivity	$W/(m \cdot K)$	33
Latent heat of fusion	J/kg	270,000
Liquidus temperature	$T_{L}(K)$	1,773
Solidus temperature	$T_{S}(K)$	1,722

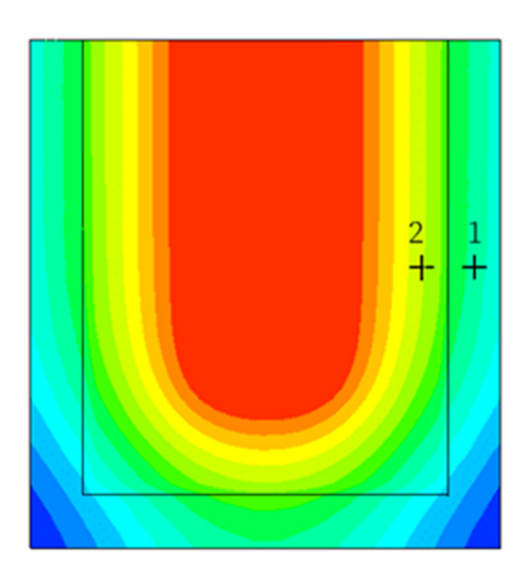


Figure 2: Locations of the temperature measuring points of the ingot.

2.4.1 Heat transfer coefficient and time

Figure 3 shows the fitting curves of the heat transfer coefficient-time variations of the ingot interfaces with 180, 380, 800, 1,300, and 1,880 mm diameters. As shown in the figure, the change trends of the heat transfer coefficients at the interfaces of the ingots with five different sizes were essentially the same. Because the initial conditions for the five ingot sizes were the same, the initial heat transfer coefficient values were relatively close and were maintained at about 4,000 W/(m².°C), despite the different diameters. When the interfacial heat transfer coefficient was above 1,000 W/(m^2 . $^{\circ}$ C), the rate of decrease was very sharp with increasing heat transfer time. This was because when the molten steel and the ingot mold were in contact, the molten steel heated the ingot mold, and due to expansion, the molten steel was subjected to rapid cooling of the ingot mold. As the temperature decreased rapidly, it shrank rapidly, forming a solidified shell, and as a result, an air gap formed between the ingot mold and ingot, which significantly reduced the heat transferability of the molten steel to the ingot mold. When the interfacial heat transfer coefficient was below 1,000 W/(m^2 .oC), the molten steel on the outer layer of the ingot was solidified, and its ability to shrink inward was much lower than that during the initial stage of solidification. At this time, the air gap between the ingot and the mold had completely formed, and the influence of the air gap on the interfacial heat transfer coefficient was no longer as obvious as during the initial stage of solidification. The ingot to ingot mold heat transfer capacity was also far lower than that during the initial stage of solidification, and the interfacial heat transfer coefficient gradually decreased and ultimately stabilized at about 100 W/(m².°C). As shown in Figure 3, with increasing ingot diameter, the rate of decrease in the interfacial heat transfer coefficient slowed. At about 2,000 s, the heat transfer coefficients of the 180 and 380 mm diameter ingots decreased to a steady state. Also, the heat transfer coefficient of the ingot interface with 800 mm diameter dropped to a stable state at about 4.000 s, the interface heat transfer coefficient of the 1,300 mm diameter ingot dropped to a steady state after about 6,000 s, and the heat transfer coefficient of the ingot interface with a diameter of 1,880 mm dropped to a stable state at about 8,000 s. This was because with an increase in ingot size, the heat dissipation rate of the ingot became slower, and the temperature drop rate slowed.

2.4.2 Interfacial heat transfer coefficient model

By observing the data in Figure 3, we found that the increases in interfacial heat transfer coefficient and heat transfer time of the ingot gradually decreased, and the variation law was close to the exponential function. The relationship between the interfacial heat transfer coefficient and the heat transfer time, corresponding to the abovementioned five ingots with different diameters, was fitted by the exponential function using data analysis software. The model of the function used for the fitting process is given by

$$h = A_1 e^{-\frac{t}{t_1}} + A_2 e^{-\frac{t}{t_2}} + B_0.$$
 (18)

The fitting results are shown by the red curve in Figure 3. Figure 3 also shows that for different diameters, the data points essentially fell near the fitting curve. By comparing the fitted interface heat transfer coefficient value with the original interface heat transfer coefficient value, it is found that the error is less than 5%, indicating that the selected function model could correctly reflect the change law of the interfacial heat transfer coefficient with time.

Taking the five time points of 500, 1,000, 2,000, 3,000, and 5,000 s, the variation law of the interfacial heat transfer coefficients corresponding to different diameters at fixed time points could be obtained, as shown in Figure 4.

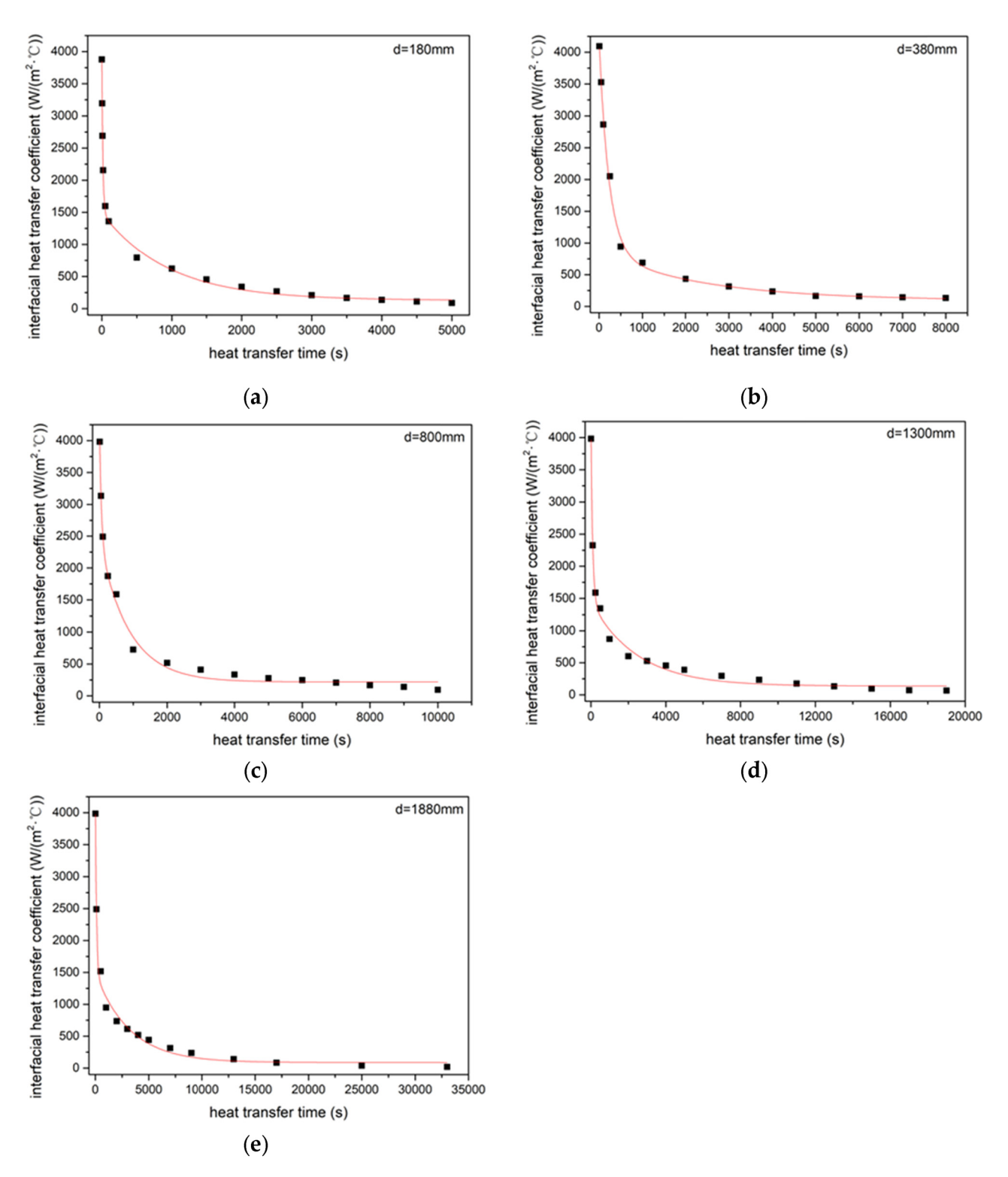


Figure 3: (a-e) The relationship between the interfacial heat transfer coefficient and time for different ingot diameters.

Figure 4 shows that at a fixed time, the interfacial heat transfer coefficient and the ingot diameter had a linear relationship, according to the following equation:

$$h = kd + b. (19)$$

Because the heat transfer coefficient of the interface conformed to equations (18) and (19), the relationship

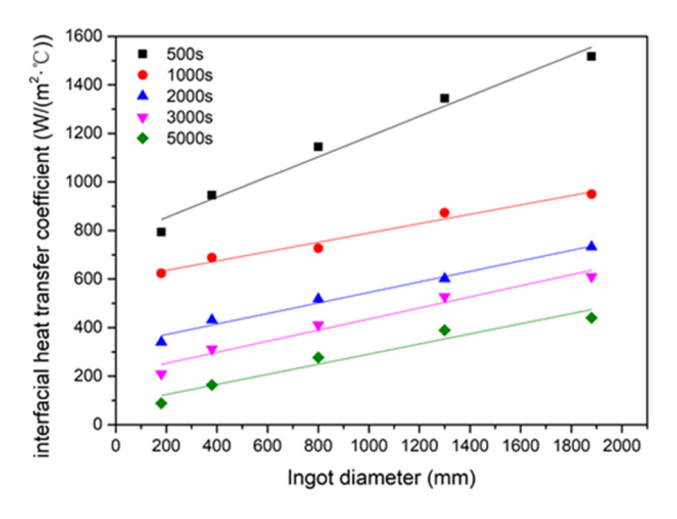


Figure 4: Changes in the interfacial heat transfer coefficient as a function of steel ingot diameter.

between the heat transfer coefficient of the interface, time, and the ingot diameter had to satisfy the following equation:

$$h = (kd + b) \times \left(A_1 e^{-\frac{t}{t_1}} + A_2 e^{-\frac{t}{t_2}} + B_0 \right). \tag{20}$$

Equation (20) was used for data regression analysis, and the relationship between the interfacial heat transfer coefficient of the ingot, the heat transfer time, and the diameter of the ingot satisfied the following equation:

$$h = (0.197d + 926.3) \times \left(1.832e^{-\frac{t}{73}} + 1.59e^{-\frac{t}{1099}} + 0.09\right). (21)$$

3 Model verification

Lan and Zhang [4] from the University of Science and Technology Beijing established a 3D finite element model of heat-fluid-force coupling during the solidification of an 8.5 tons ingot. The cross-sectional area of the middle height of the ingot is $0.7825 \times 0.6825 \,\mathrm{m}^2$, and the pouring temperature is 1,520°C [5]. The author used Procast to inversely calculate the interface heat transfer coefficient between the ingot and the ingot mold, and the temperature change of the ingot and the ingot mold calculated by using the result was basically consistent with the measured value. Since the cross-sectional area of the steel ingot in this article is square, when the diameter of the steel ingot is 820 mm, the cross-sectional area is consistent with the model in the literature. Entering d = 820 mminto equation (21) could obtain the interface heat transfer coefficient curve of the 820 mm diameter steel ingot as a function of time, as shown in Figure 5.

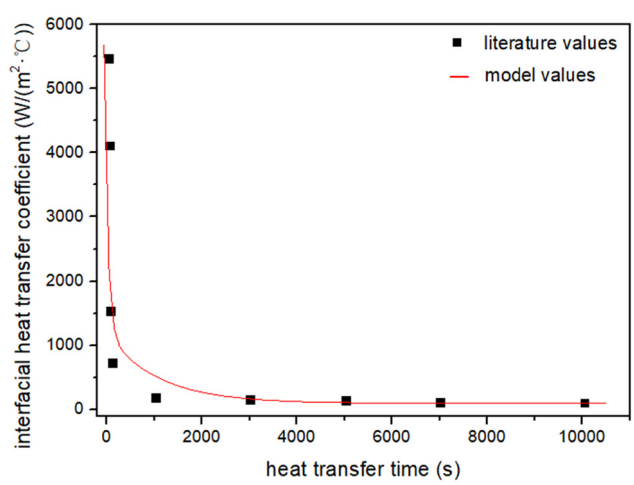


Figure 5: Interfacial heat transfer coefficient of an 820 mm diameter ingot.

As shown in Figure 5, the trend of the model value of the interface heat transfer coefficient calculated by equation (21) is basically consistent with the value in the literature. When the interface heat transfer coefficient is reduced to 1,000 W/(m^2 .°C), the decline rate of the model value is slightly slower than the literature value. By about 3,000 s, the model value and the literature value are reduced to about 150 W/(m^2 .°C), and the law of change between the two is basically the same.

Tu [17] from Tsinghua University inversed the changes in interfacial heat transfer coefficient between the ingot and the ingot mold with time by actually measuring the temperature changes during the cooling process of ingot pouring. The weight of the ingot was about 36 tons, the average diameter of the ingot body was 1,500 mm, the pouring temperature was 1,560°C, and the surface of the molten steel was covered with a layer of insulation agent after pouring. After inputting d = 1,500 mm into equation (21), the interfacial heat transfer coefficient curve for the 1,500 mm diameter steel ingot as a function of time could be obtained, as shown in Figure 6.

As shown in Figure 6, at the beginning of heat transfer, the model value was very close to the literature value, with both at about $4,000\,\mathrm{W/(m^2\cdot^0C)}$. Between 0 and $1,000\,\mathrm{s}$, both the literature and model values decreased very rapidly, corresponding to the formation of an air gap between the ingot and the ingot mold. At $1,000\,\mathrm{s}$, the literature value decreased to $1,000\,\mathrm{W/(m^2\cdot^0C)}$, and the model value decreased to $892\,\mathrm{W/(m^2\cdot^0C)}$. When the interfacial heat transfer coefficient was below $1,000\,\mathrm{W/(m^2\cdot^0C)}$, the decline rate for the model was slightly slower than that for the literature values. By about $5,000\,\mathrm{s}$, the air gap between the ingot and the ingot mold reached a stable stage, and

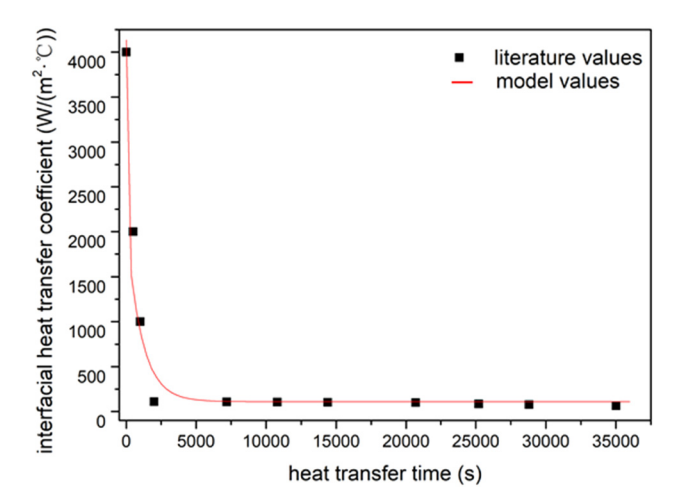


Figure 6: Interfacial heat transfer coefficient of a 1,500 mm diameter ingot.

at this time, the model and literature values decreased to $100-110~\text{W/(m}^2\cdot^{\circ}\text{C})$. With an increase in heat transfer time, these values essentially did not change. Between 20,000~and~35,000~s, the literature values started to decline slowly, but throughout the entire solidification stage, the change trends of the model values were essentially consistent with those of the literature values.

Considering that the heat transfer coefficient for the ingot solidification interface can be affected by many factors, such as the pouring temperature, ingot mold thickness, molten steel composition, and the surface roughness of the ingot mold, errors between the model and literature values were within a reasonable range. Therefore, equation (21) could correctly express the interfacial heat transfer coefficient between the ingot and ingot mold.

4 Conclusions

- 1. In this study, we established 3D models of ingots with different sizes, and the change laws of the interfacial heat transfer coefficients between the ingots and ingot molds with different sizes were analyzed using Fluent finite element analysis software. We found that the change law for the interfacial heat transfer coefficient of ingots with all sizes as a function of time conformed to the change law of the exponential function. Furthermore, the interfacial heat transfer coefficient and the ingot diameter had a linear relationship
- 2. This proved that the relationship between the heat transfer coefficient at the ingot interface, the heat

transfer time, and the ingot diameter was satisfied $h = (0.197d + 926.3) \times \left(1.832e^{-\frac{t}{13}} + 1.59e^{-\frac{t}{1099}} + 0.09\right)$. In the initial stage of solidification, the interfacial heat transfer coefficient decreased rapidly. When it decreased below 1,000 W/(m².°C), the rate of decrease became slightly slower. When the interfacial heat transfer coefficient decreased to 100-150 W/(m².°C), and with an increase in heat transfer time, essentially no changes were observed.

Acknowledgement: The authors gratefully acknowledge financial support from State Key Laboratory of advanced metallurgy (No. k22-10), Fundamental Research Program of Shanxi Province (No. 20210302123218, No. 202103021223277), Taiyuan University of Science and Technology Doctoral Research Fund (No. 20212025), and Research Project Supported by Shanxi Scholarship Council of China (HGKY2019084).

Funding information: This research was funded by State Key Laboratory of advanced metallurgy (No. k22-10), Fundamental Research Program of Shanxi Province (No. 20210302123218, No. 202103021223277), Taiyuan University of Science and Technology Doctoral Research Fund (No. 20212025), and Research Project Supported by Shanxi Scholarship Council of China (HGKY2019084).

Author contributions: Writing – original draft preparation, software, validation, investigation, data curation, visualization: Yukun Zhao; conceptualization, methodology, project administration, funding acquisition: Yihong Li; writing – review and editing, supervision: Huiqin Chen.

Conflict of interest: The authors declare no conflict of interest.

Data availability statement: All authors can confirm that all data used in this article can be published in High Temperature Materials and Processes.

References

- [1] Li, W. M., Y. F. Geng, X. M. Zang, Y. A. Jing, D. J. Li, and B. G. Thomas. Air gap measurement during steel-ingot casting and its effect on interfacial heat transfer. *Metallurgical and Materials Transactions B*, Vol. 52, 2021, pp. 2224–2238.
- [2] Muojekwu, C. A., I. V. Samarasekera, and J. K. Brimacombe. Heat transfer and microstructure during the early stages of

- metal solidification. *Metallurgical and Materials Transactions B*, Vol. 26, No. 2, 1995, pp. 361–382.
- [3] Kumar, T. S. P. and K. N. Prabhu. Heat flux transients at the casting/chill interfacial during solidification of aluminum base alloys. *Metallurgical and Materials Transactions B*, Vol. 22B, No. 10, 1991, pp. 717–727.
- [4] Lan, P. and J. Q. Zhang. Numerical analysis of interfacial heat transfer coefficient during large steel ingot solidification. *Journal of Iron and Steel Research*, Vol. 26, No. 8, 2014, pp. 29–36.
- [5] Lan, P. and J. Q. Zhang. Numerical analysis of macrosegregation and shrinkage porosity in large steel ingot. *Ironmak & Steelmak*, Vol. 41, No. 8, 2014, pp. 598–606.
- [6] Zeng, Y. D., Q. H. Yao, and X. Wang. The effect of air gap between casting and water-cooled mold on interface heat transfer coefficient. *Materials Science Forum*, Vol. 893, 2017, pp. 174–180.
- [7] Guo, Z. P., S. M. Xiong, S. X. Cao, and Z. J. Cui. Effects of alloy materials and process parameters on the heat transfer coefficient at metal/die interface in high pressure die casting. *Acta Metallurgica Sinica*, Vol. 4, 2008, pp. 433–439.
- [8] Wang, J. Q., P. X. Fu, H. W. Liu, D. Z. Li, and Y. Y. Li. Shrinkage porosity criteria and optimized design of a 100-ton 30Cr2Ni4MoV forging ingot. *Materials & Design*, Vol. 35, 2012, pp. 446–456.
- [9] Li, W. S., H. F. Shen, and B. C. Liu. Three-dimensional simulation of thermosolutal convection and macrosegregation

- in steel ingots. *Steel Research International*, Vol. 81, No. 11, 2010, pp. 994–1000.
- [10] Liu, D. R., D. Z. Li, and B. G. Sang. Numerical simulation of macrosegregation for an Fe-0.8 wt pct C alloy. *Journal of Materials Science and Technology*, Vol. 25, No. 4, 2009, pp. 561–568.
- [11] Li, Q., C. L. Mo, X. H. Kang, D. Z. Li, and B. N. Qian. Numerical simulation of the influence of heat extract boundary conditions and densities on the thermo-solutal convection. *Materials Science and Technology*, Vol. 1, 2005, pp. 94–98.
- [12] Wu, K. *Metallurgy transport principle*. 2rd ed. Metallurgical Industry Press: Beijing, China, 2016, pp. 133-239.
- [13] Mustafa, R. O., X. L. Hong, and X. T. Lu. Experimental and mathematical studies on bloom solidification, die wall deflection and ingot-die air gap formation. *Baotou Steel Science and Technology*, Vol. 2, 1987, pp. 55–66.
- [14] Zhu, L. P. Study on heat transfer coefficients at metal/mold interface during solidification in metal castings. Master's thesis. Tianjin University of Technology, Tianjin, 2009.
- [15] Ma, W. Study on solidification process of super-huge steel ingot. Master's thesis, Chongqing University, Chongqing, 2011.
- [16] Zhao, B. The numerical simulation of macrosegregation and stress field during solidification of super large steel ingot. Master's thesis, Chongqing University, Chongqing, 2013.
- [17] Tu, W. T. Modelling and simulation of macrosegregation in large steel ingots by multicomponent and multi phase model.

 Doctoral dissertation. Tsinghua University, Beijing, 2016.